Burns & Trauma, 2021, 9, tkab010
https://doi.org/10.1093/burnst/tkab010
Research Article

Research Article

Low-protein diet accelerates wound healing in mice post-acute injury

Jonathan J. Hew[1,†], Roxanne J. Parungao[1,†], Craig P. Mooney[1], Julian K. Smyth[1], Sarah Kim[2], Kevin H.-Y. Tsai[3], Huaikai Shi[1], Cassandra Chong[1], Renee C. F. Chan[4], Beba Attia[4], Caroline Nicholls[5], Zhe Li[1,5], Samantha M. Solon-Biet[6,7], David G. Le Couteur[6], Stephen J. Simpson[7], Marc G. Jeschke[8], Peter K. Maitz[1,5] and Yiwei Wang[1,9,*]

[1]Burns Research and Reconstructive Surgery, ANZAC Research Institute, Concord Hospital, University of Sydney, Sydney, Australia 2139, [2]Bone Biology Group, ANZAC Research Institute, Concord Hospital, University of Sydney, Sydney, Australia 2139, [3]Adrenal Steroids Laboratory, ANZAC Research Institute, Concord Hospital, University of Sydney, Sydney, Australia 2139, [4]Electron Microscopy Unit, Anatomical Pathology, Concord Hospital, Sydney, Australia 2139, [5]Burns Unit, Concord Repatriation General Hospital, Concord, Australia 2139, [6]Ageing and Alzheimer Institute and ANZAC Research Institute, Concord Hospital, University of Sydney, Sydney, Australia 2139, [7]Charles Perkins Centre and School of Life and Environmental Sciences, University of Sydney, Australia 2006, [8]Sunnybrook Research Institute, Toronto, Ontario, Canada, M4N 3M5 and [9]School of Pharmacy, Nanjing University of Chinese Medicine, Nanjing, PR China 210023

*Correspondence. Email: yiweiwang@anzac.edu.au, yiweiwang@njucm.edu.cn

[†]Equal contribution.

Received 8 October 2020; Revised 6 December 2020; Accepted 11 March 2021

Abstract

Background: Wound healing processes are influenced by macronutrient intake (protein, carbohydrate and fat). The most favourable diet for cutaneous wound healing is not known, although high-protein diets are currently favoured clinically. This experimental study investigates the optimal macronutrient balance for cutaneous wound healing using a mouse model and the Geometric Framework, a nutrient modelling method, capable of analyzing the individual and interactive effects of a wide spectrum of macronutrient intake.

Methods: Two adjacent and identical full-thickness skin excisions (1 cm^2) were surgically created on the dorsal area of male C57BL/6 mice. Mice were then allocated to one of 12 high-energy diets that varied in protein, carbohydrate and fat content. In select diets, wound healing processes, cytokine expression, energy expenditure, body composition, muscle and fat reserves were assessed.

Results: Using the Geometric Framework, we show that a low-protein intake, coupled with a balanced intake of carbohydrate and fat is optimal for wound healing. Mice fed a low-protein diet progressed quickly through wound healing stages with favourable wound inflammatory cytokine expression and significantly accelerated collagen production. These local processes were associated with an increased early systemic inflammatory response and a higher overall energy expenditure, related to metabolic changes occurring in key macronutrient reserves in lean body mass and fat depots.

Conclusions: The results suggest that a low-protein diet may have a greater potential to accelerate wound healing than the current clinically used high-protein diets.

Key words: Wound healing, Macronutrients, Cutaneous, Geometric Framework, Mouse model, Low-protein diet, Nutrition

Highlights

- A low-protein diet paired with a balanced carbohydrate and fat intake accelerates cutaneous wound healing in mice.
- Faster wound healing is associated with enhanced collagen deposition and an early but short inflammatory response.
- Faster wound healing is found to be associated with a higher overall energy expenditure.
- Identified potential endogenous dietary pathways involved in wound healing for future investigation.

Background

Wound healing is a common surgical issue in which simple interventions, such as nutritional support, can make a major difference. Macronutrients (protein, carbohydrate and fat) are energy-providing dietary components [1]. It is well known that adequate macronutrient intake is essential for healing, as wounds require additional energy and substrates for anabolic processes [2]. During wound healing, protein in the form of amino acids is essential for the formation of new tissues, gluconeogenesis and protein synthesis [3]. Carbohydrates are a protein-sparing energy source required by epithelial, inflammatory and immune cells [4]. Fats are a dense energy source and have additional roles as signalling molecules and as components of the cell membrane [5].

High-protein diets are believed to accelerate wound healing by supporting protein-demanding healing processes, while minimizing depletion of valuable intrinsic protein reserves, particularly lean mass [2,6,7]. For this reason, high-protein diets are used routinely to support healing of simple surgical wounds, complex chronic wounds, in enhanced recovery after surgery protocols and burns [8,9]. In previous studies, investigating the role of macronutrients in wound healing has been limited by a narrow methodology that involved manipulating single nutritional components e.g. protein or fat. In this study, this limitation is addressed by using the Geometric Framework (GF), a complete method of analysis that is capable of modelling the simultaneous, individual and interactive effects of macronutrients [10]. The aim of this study was to firstly use the GF to identify the most favourable dietary balance of protein, carbohydrate and fat for wound healing in a C57BL/6 mouse model. The second aim was to identify potential local and systemic processes influenced by macronutrient intake that may affect wound healing. Identifying these relationships is essential to guide future research aimed at uncovering the complex local and systemic mechanisms by which variations in the dietary intake of protein, carbohydrate and fat can enhance wound healing.

Methods

Experimental models and subject details

Male C57BL/6 mice (Animal Resource Centre, Western Australia; 4 weeks old, 19.75 ± 1.01 g, number = 336; $n = 3$ mice/diet/time point and $n = 6$ mice/diet/time point in select diets; additional mice added for further investigation in these groups) were housed three per cage in standard approved cages with free access to water in a specific-pathogen-free facility. The environment was closely controlled at 24–26°C and 44–46% humidity under a 12:12 h light/dark cycle with lights on at 6 am. All protocols were approved by the Sydney Local Health District Welfare Committee (Protocol No. 2014/013) under Australian National Health and Medical Research Council Guidelines for animal experimentation. Mice were fed with standard chow for 8 weeks. After an 8-week feeding period, mice were anaesthetized with ketamine/xylazine (0.1 mL/20 g, contains 87.5 mg/12.5 mg/kg) and two adjacent but identical full-thickness skin excisions of 1 cm^2 (representing 5% total body surface area) were created surgically on the dorsal area. The wound area was covered with dressings that were replaced as needed in the first 7 days post-injury. Analgesia (intraperitoneal carprofen 5 mg/kg) was provided daily for 2 days after skin excision. Warm resuscitative intraperitoneal saline (1 mL) was given immediately after surgery. Mice were monitored daily for the first 7 days for any signs of distress by measuring changes in body weight and assessing any changes in physical appearance and behaviour. The survival or cause-specific mortality rate of animals was recorded and calculated by the time interval of death.

Post-surgery, all animals were separated into individual cages and randomly allocated to one of 12 high-energy diets to feed *ad libitum*. The diets varied in protein (5–60%, casein and methionine), carbohydrate (20–75%, sucrose, wheat-starch and dextrinized cornstarch) and fat (20–75%, soya bean oil) content (Table S1) (Specialty Feeds, Glen Forest, WA). Diets were systematically designed for optimal power in fitting surface response models and to have a high-energy

density of 17 kJ g^{-1} (Figure S1, see online supplementary material). Two additional diets based on current popular clinical ratios, a high-protein, high-carbohydrate (HPHC) and a high-protein, high-fat (HPHF) diet, were also tested [11].

During the healing process, body composition was assessed weekly using an in-house Dual- Energy X-ray Absorptiometry (DEXA) scanner. Wound healing rate was measured using VISITRACK™ (Smith & Nephew, London, UK). At each time point (D3, D7, D14, D21, where D is day), mice were anaesthetized using a cocktail of ketamine/xylazine (100 mg/kg ketamine/100 mg/kg xylazine), blood was collected via cardiac puncture and mice were euthanized by cervical dislocation. Wound, extensor digitorum longus muscle (EDL), inguinal white adipose tissue (iWAT) and brown adipose tissue (BAT) tissue were harvested, and were either fixed in 10% formalin for histological analysis or immediately frozen for molecular analysis.

Histological analysis

Wounds were embedded in paraffin and multiple 5 µm sections were stained with haematoxylin and eosin (H&E) for general histological analysis and Masson's Trichrome for collagen deposition.

Immunohistochemistry

Wound sections were stained for proliferating cell nuclear antigen (PCNA) (Invitrogen, Carlsbad, CA) to measure cell proliferation. On the same slides, epidermal migration was measured using OsteoMeasureXP. Multiple 5 µm sections of iWAT and BAT were incubated with anti-uncoupling protein-1 (anti-UCP-1) antibody (Abcam, Cambridge). Images were taken with an EVOS cell imaging system (Thermo Fisher Scientific, Waltham, MA).

Transmission electron microscopy analysis

EDL muscle was fixed in 10% formalin. The specimen was placed in 0.1 M sodium cacodylate buffer, post-fixed in 2% osmium tetroxide and treated with 0.5% uranyl acetate. The specimen was dehydrated through a graded series of ethanol, placed in acetone, infiltrated in 50:50 acetone: Spurr's resin, then embedded in pure Spurr's resin and polymerized overnight at 70°C. Semi-thin sections (0.5 µm) were stained with toluidine blue and examined by light microscopy to select appropriate areas for ultrastructural examination. Ultrathin sections of 90 nm were contrast-stained with uranyl acetate and lead citrate and examined using a Fei Tecnai Spirit Biotwin electron microscope. Images were obtained with an Olympus-SIS veleta digital camera.

Real time-quantitative polymerase chain reaction

RNA from wound, adipose tissue (iWAT and BAT) and EDL muscle were extracted with TRI Reagent (Sigma Aldrich, St. Louis, MO). Total RNA (1 µg) was reverse transcribed. Primers (Table S4) were designed using Primer-BLAST Software. Real time-quantitative PCR (RT-qPCR) was performed using SYBR Green Supermix (Bio-Rad, Hercules, CA). mRNA expression was quantified using the $2^{-\Delta\Delta^{Ct}}$ method and normalized against ribosomal protein L19 (RPL19) and peptidylprolyl isomerase A (PPIA) housekeeping genes.

Cytokine expression

The Bio-Plex Pro™ Mouse Cytokine 23-plex Assay (Bio-Rad) was used to profile the expression of 23 inflammatory mediators from terminal blood samples collected via cardiac puncture. The assay was performed according to the manufacturer's instructions.

Metabolism

Following injury, mice were housed individually in Promethion metabolic cage systems (Sable Systems International, Las Vegas, NV). Mice were housed in the metabolic cages throughout the wound healing process, where gas exchange, energy expenditure and total activity (allmeters/pedmeters) were continuously measured. The respiratory exchange quotient (RQ) was calculated as a ratio of CO_2 production over O_2 consumption and was used as an indicator of substrate utilization. An RQ of 1.0 indicates primarily carbohydrate metabolism, 0.8 mixed carbohydrate and fat metabolism and 0.7 primarily fat metabolism. Energy expenditure was calculated using the Weir equation [12]: $\text{Kcal/h} = 60 \times (0.003941 \times VO_2 + 0.001106 \times VCO_2)$.

Statistical analysis

Generalized additive models (GAM) were constructed for this study. Response surfaces were generated using non-parametric thin plate splines in R (v3.4.3) and analyzed using GAM. Statistical analyses for individual diets were performed using IBM SPSS V25 using generalized estimating equations (GEE). Data are presented as mean ± standard error of mean. Mortality was displayed as a Kaplan–Meier curve with log rank test and pairwise comparisons. Statistics for food intake were calculated with one-way ANOVA and Tukey's *post hoc* test.

Justification of sample size: $n = 6$/group per time point gave us 98% power for two-sided α ($p = 0.05$) to detect ≥20% difference in wound healing rate. For GF, greater sensitivity allows for fewer mice with 3 of each diet required to detect differences of ≥10% in wound healing.

Results

The effect of macronutrient intake on cutaneous wound healing

Response surfaces were generated from all surviving mice at each time-point, and the main and interactive effects of protein, fat and carbohydrate intake were tested statistically using general additive modelling (Tables S2 and S3). Wound healing was optimized with a low-protein, high carbohydrate and/or fat intake, and delayed by a high-protein or a very

high-fat intake. This was demonstrated on D3 and D7, with mice consuming carbohydrate to fat in a ratio between 1:1 and 5:1 having 20% wound closure by D3 and 60% by D7 (Figure 1a and b). At D14, mice consuming a carbohydrate to fat ratio closer to 1:1 had improved wound healing at 90%, compared to 75% with a 5:1 carbohydrate to fat ratio (Figure 1c). This indicates that non-protein energy should preferably come from a balanced intake of fat and carbohydrate. Delayed wound healing occurred in mice with high-protein intakes, achieving only 50% wound closure on D14 when mice consumed >30 kJ/day of protein (Figure 1c). Very high-fat intake severely delayed wound healing, with mice consuming 50 kJ/day (80% energy intake) showing healing of 5% on D3 and 40% on D7 (Figure 1a and b).

Individual analysis of dietary groups supported response surface findings. Diets are named firstly according to the amount of protein (H = high, M = moderate, L = low) and secondly by the macronutrient providing the majority of calories (P = protein, C = carbohydrate, F = fat, CF = carbohydrate and fat equivalent). From the 12 screened diets, healing was similar and fastest in the low-protein diets (Table S1 and Figure S1). The low-protein, equivalent carbohydrate and fat (LPCF, P5:C48:F48) diet was selected as the optimal diet because the C:F ratio was 1:1 as per the response surface analysis for D14 wound healing (Figure 1c). In comparison to the optimal LPCF diet, which had 94% wound closure by D14, the clinical control, HPHC diet (P26:C57:F17) had 78% wound closure by D14 (Figure 1d). Wound healing was poorest in the moderate-protein, low-carbohydrate, high-fat diet (MPHF, P14:C29:F57), with 45% wound closure on D14 (Figure 1d). These results are represented in Figure 1(e) which demonstrates accelerated wound healing in LPCF and HPHC mice and delayed healing in MPHF mice. Mice fed these three diets (LPCF, HPHC and MPHF) represented the optimal, clinical control and poorest diets, and were selected for further analysis to identify potential local and systemic mechanisms responsible for the observed difference in wound healing. In the primary cohort of mice, a high mortality rate of ~47% (7/15 mice) was observed in the MPHF group due to weight loss and failure to heal (Figure 1f), and 1/15 deaths in the LPCF group. Overall there was no significant difference in mortality between LPCF and HPHC groups.

Macronutrient intake and local healing processes

The inflammatory (D3–7), proliferative (D7–14) and remodelling (D14–21) phases of wound healing were assessed in select diet groups (LPCF, HPHC, MPHF). H&E staining showed increased inflammatory cells in the HPHC wound sections (Figure 2a), which is supported by the significantly higher mRNA expression of inflammatory cytokines, IL-6 and TNF-α on D3 (Figure 2b and c). MPHF sections showed adipocyte migration into the wound bed with poor epidermal migration and consistently reduced expression of IL-6 and TNF-α on D3 (Figure 2a–d). In contrast, LPCF staining showed improved epidermal migration, well organized epithelial tongues and a moderate density of inflammatory cells (Figure 2a). On D7, the mRNA expression of IL-6, TNF-α and TGF-β1 in LPCF mice was increased in wound tissue (Figure 2b–d).

Epidermal tongue length showed a trend towards enhanced migration (~328 μm) in the LPCF sections when compared to HPHC (~243 μm) and MPHF (~286 μm) on D7 (Figure 2e and f). On D14, greater cell proliferation was observed in diets with higher carbohydrate composition, with ~95% in LPCF and ~94% in HPHC sections compared to a lesser but not significant ~84% in MPHF (Figure 2f and g). Masson's trichrome staining of D14 wounds generally showed increased deposition of collagen in LPCF wounds, with more prominent staining of green collagen fibres (Figure 2h). This finding is supported by the increased mRNA expression of collagen III and collagen I in LPCF wounds on D7, indicating early and advanced collagen deposition (Figure 2i and j). Furthermore, collagen III and I mRNA expression in LPCF wounds continued to decline, indicating a resolving remodelling phase and wound maturation. Following a similar but delayed pattern, mRNA expression of collagen III and I in HPHC wounds peaked on D14 then declined, while in MPHF wounds, the mRNA expression of collagen III and I remained low throughout the healing process (Figure 2i and j).

Systemic cytokine response to injury

Systemic cytokine levels were measured on D3 and D7 to assess the effect of macronutrients on the systemic inflammatory response syndrome (SIRS) after injury. Of the 23 cytokines, 17 were elevated in LPCF mice on D3, including key cytokines such as IL-6, IL-1, IL-12, TNF-α and INF-λ (Figure 3). Most cytokines had returned to baseline levels by D7 in the LPCF and MPHF groups, indicating cessation of the SIRS response to injury. In contrast, the HPHC group continued to demonstrate increased levels, suggesting a prolonged SIRS response to injury.

Metabolic response to injury and macronutrient intake

A RQ of >0.8 confirmed that mice consuming HPHC derived energy primarily from carbohydrates, LPCF mice (RQ ~0.8) from a mixed diet and MPHF mice (RQ < 0.8) from fat (Figure 4a and b). Energy expenditure increased during the day and night compared to baseline (pre-injury) in all groups after injury, and returned to baseline by D14 in MPHF and HPHC mice. Energy expenditure in LPHC mice was significantly greater and prolonged (Figure 4c and d). Total movement was similar between all groups (Figure 4e and f).

The mean intake of individual macronutrients was significantly different between groups, with HPHC mice consuming the most protein at ~15 kJ/day compared to ~8 and ~4 kJ/day in MPHF and LPCF mice, respectively. HPHC and LPCF mice had a greater carbohydrate intake with ~34 and ~38 kJ/day, respectively compared to MPHF

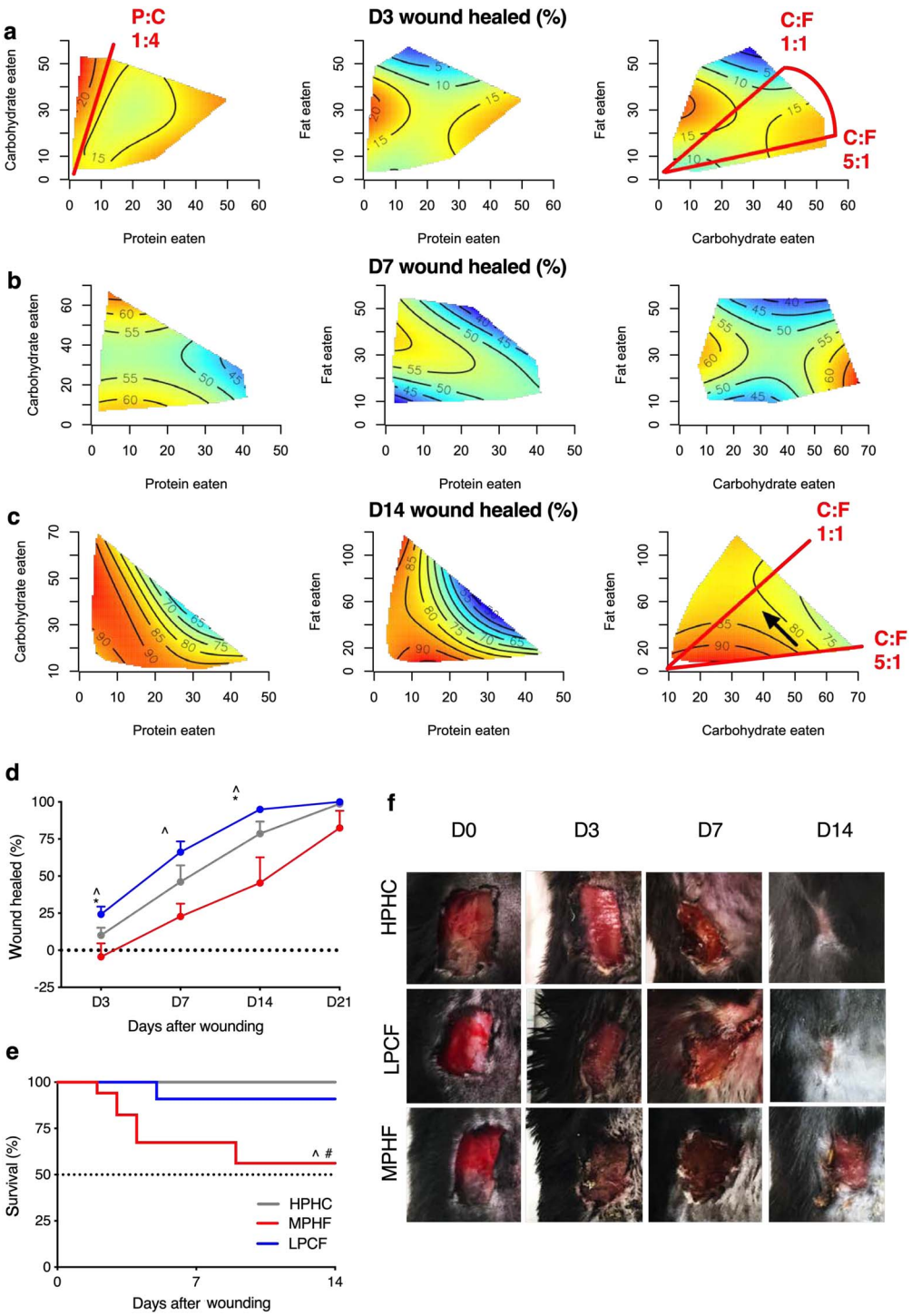

Figure 1. The effect of macronutrient intake on cutaneous wound healing. (**a-c**) Response surfaces showing the effect of macronutrient intake (kJ/day) on wound healing for D3, D7 and D14 after injury. The solid red lines indicate a nutritional rail with a fixed ratio of macronutrients. Black arrow points toward optimal intakes on D14. (**d**) Wound healing rate, (**e**) representative images of dorsal wounds healing and (**f**) Kaplan–Meier curve showing mortality rate in select diets (LPCF, MPHF and HPHC). Data presented as mean ± SEM. #$p \leq 0.05$ HPHC *vs* MPHF, *$p \leq 0.05$ LPCF *vs* HPHC, ^$p \leq 0.05$ LPCF *vs* MPHF. $n = 6$ for each group. Black dotted lines indicate the base line level. (Table S2). *LPCF* low protein, equivalent carbohydrate and fat diet, *HPHC* high-protein, high-carbohydrate diet, *MPHC* moderate-protein, low-carbohydrate, high fat diet

mice at ~17 kJ/day. Both LPCF and MPHF mice consumed more fat, ~33 and ~38 kJ/day respectively, compared to HPHC at ~11 kJ/day (Figure 4g). Energy intake was higher on average in LPCF mice that consumed ~80 kJ/day over the period of wound healing, compared to ~60 kJ/day in HPHC and MPHF (Figure 4g).

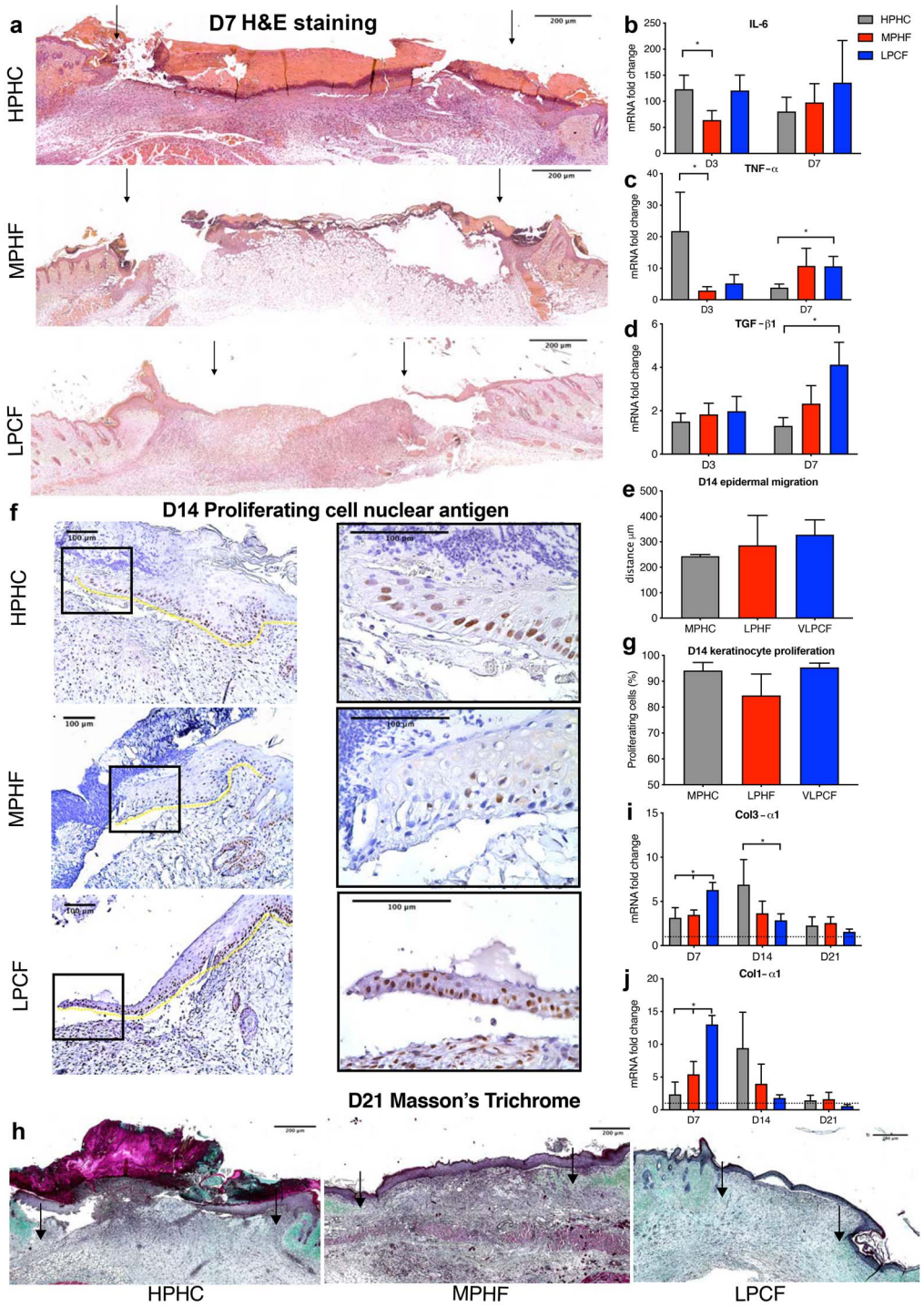

Figure 2. Macronutrient intake effects on local healing processes. Analysis of wounds at different stages of wound healing, inflammatory (**a**–**d**), proliferative (**e**–**g**) and remodelling (**h**–**j**). (a) H&E staining of D7 wounds, arrows indicate the edge of the migrating epithelial tongue (scale bar = 200 µm). (b–d) Wound mRNA expression of inflammatory cytokines on D3 and D7. (f) Proliferating cell nuclear antigen (PCNA) immunohistochemical staining of D14 wounds, yellow dotted line along basement membrane with positive (brown) and negative (blue) cells (scale bar = 100 µm). (g) % PCNA positive keratinocytes in D14 wounds. (h) Masson's trichrome staining of D21 wounds, collagen fibers staining green shown by black arrows (scale bar = 200 µm). (i) Collagen type III alpha 1 chain (Col3α1) and (j) collagen type I alpha 1 chain (Col1α1) mRNA expression in D7, D14 and D21 wounds. $*p \leq 0.05$, $n = 6$. Black dotted lines indicate mRNA levels in non-injured control mice. *LPCF* low protein, equivalent carbohydrate and fat diet, *HPHC* high-protein, high-carbohydrate diet, *MPHF* moderate-protein, low-carbohydrate, high fat diet

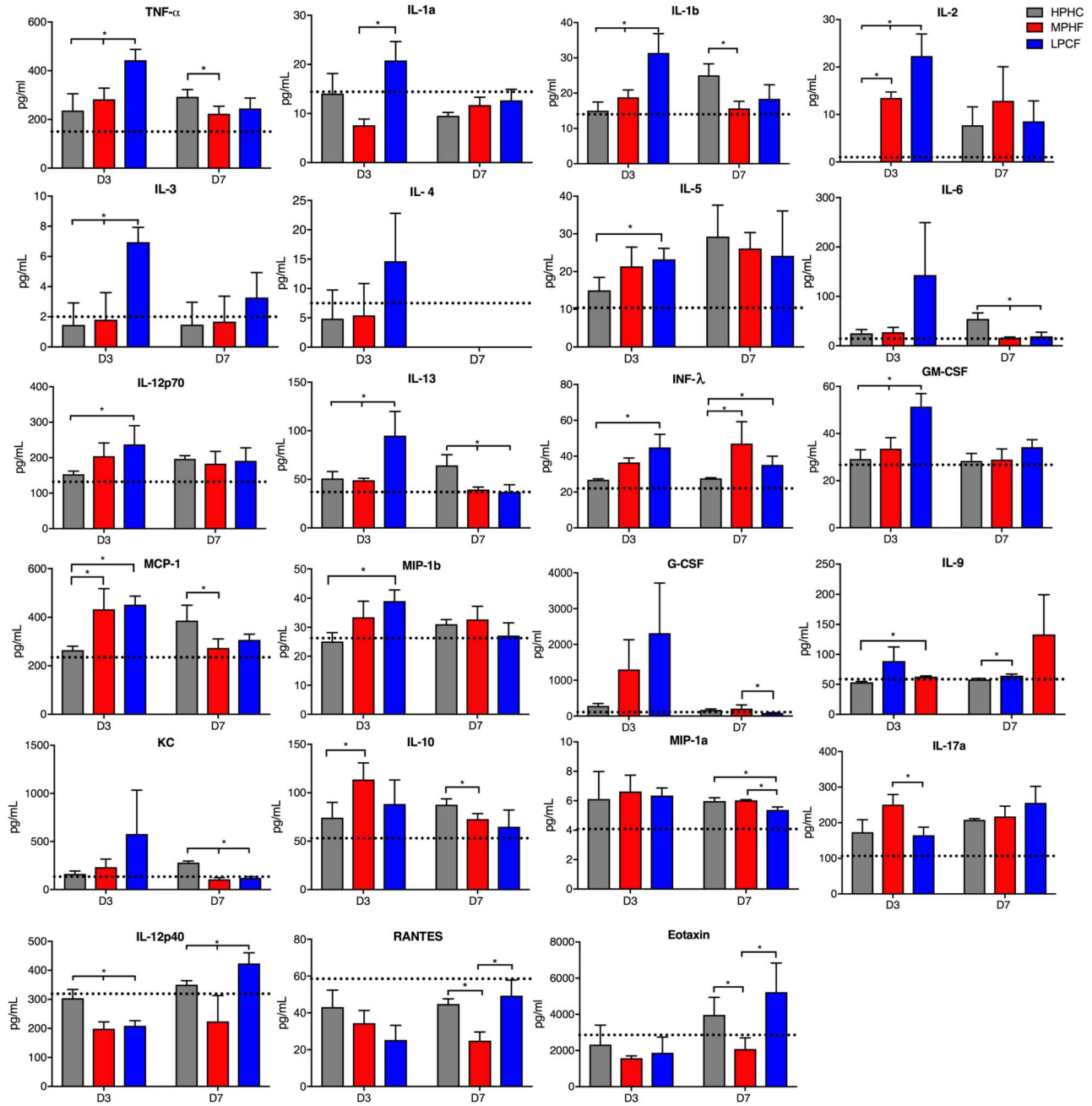

Figure 3. Cytokine response to full-thickness skin excision injury of mice. Mouse cytokine 23-plex assay results showing inflammatory cytokines regulating the systemic inflammatory response syndrome (SIRS) response (IL-1, IL-6, IL-12, TNF-α, INF-λ) and compensatory anti-inflammatory response syndrome (CARS) (IL-10, IL-4). 17/23 cytokines elevated in LPCF mice on day 3 and 9/23 elevated in HPHC mice on day 7. Data presented as mean ± SEM, black dotted lines indicate cytokine levels in non-injured control mice, $n = 3$/diet. $^{*}p \leq 0.05$. *IL* interleukin, *TNF* tumor necrosis factor, *INF* interferon, *GM-CSF* granulocyte-macrophage colony-stimulating factor, *MCP* monocyte chemoattractant protein, *G-CSF* granulocye colony stimulating factor, *KC* keratinocytes-derived chemokine, *MIP* macrophage inflammatory proteinprotein, *RANTES* regulated upon activation normal T cell expressed and secreted factor, *LPCF* low protein, equivalent carbohydrate and fat diet, *HPHC* high-protein, high-carbohydrate diet, *MPHF* moderate-protein, low-carbohydrate, high fat diet

Systemic effect of macronutrient intake on fat and lean mass

By D21 post-injury, HPHC mice gained ~2.5% body weight, while MPHF mice lost ~2% and LPCF mice lost ~5% (Figure 5a). Mice fed a LPCF diet gained ~10% fat mass compared to MPHF who gained ~1.5% fat mass and HPHC with no change (Figure 5b). This was supported by a small increase in iWAT mass and a significant increase in BAT tissue mass in LPCF mice (Figure 5c and d). To assess thermogenesis, uncoupling protein-1 (UCP-1) protein expression in BAT and iWAT tissue was measured. On D21, UCP-1 mRNA expression was increased in iWAT (~1060-fold) and BAT (~1.3-fold) tissue of LPCF mice, suggesting increased thermogenesis when compared to MPHF (~315 and ~0.9-fold, iWAT and BAT, respectively) and HPHC (~550 and 1.0-fold, iWAT and BAT, respectively) (Figure 5e and f).

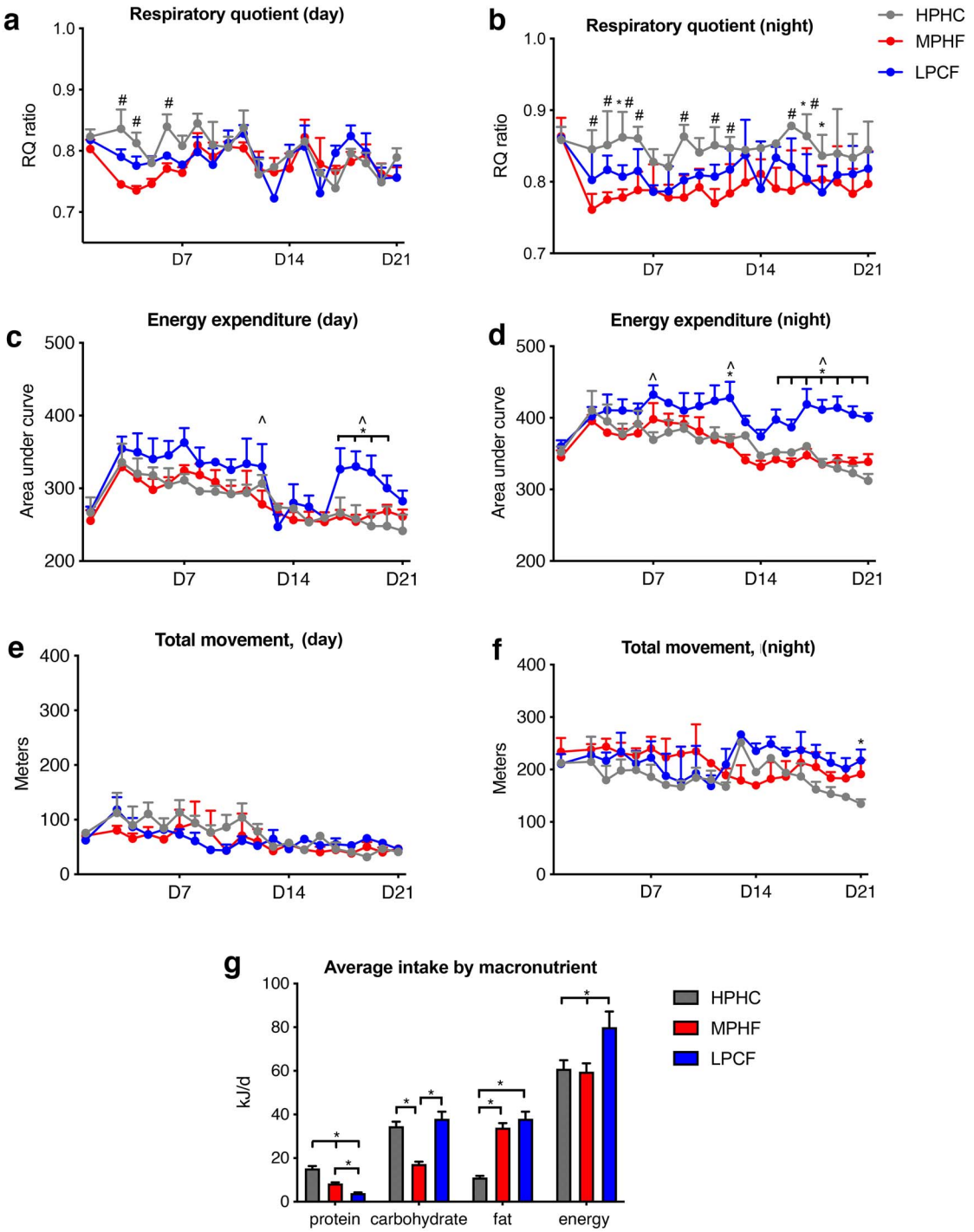

Figure 4. Metabolic cage studies and food intake of mice after full-thickness skin excision injury. (**a**, **b**) Respiratory quotient during the day and night, (**c**, **d**) energy expenditure during the day and night, (**e**, **f**) pedmeters during the day and night and (**g**) average macronutrient and energy intake over wound healing period in select diets (HPHC, MPHF and LPCF). #$p \leq 0.05$ HPHC *vs* MPHF, *$p \leq 0.05$ LPCF *vs* HPHC, ^$p \leq 0.05$ LPCF *vs* MPHF. Data presented as mean ± SEM, $n = 3$ mice/metabolic cage diet, $n = 6$/diet for energy intake. *LPCF* low protein, equivalent carbohydrate and fat diet, *HPHC* high-protein, high-carbohydrate diet, *MPHF* moderate-protein, low-carbohydrate, high fat diet

Immunohistochemical staining for UCP-1 confirmed browning of iWAT, with higher UCP-1 protein expression and multilocular adipocytes in iWAT of LPCF mice (Figure 5g). UCP-1 staining in brown fat showed a generally dense expression in all diets as expected (Figure 5h).

Similarly to body weight, by D21 HPHC mice gained ∼3.5% lean mass, while MPHF and LPCF mice lost ∼5% (Figure 5i). The EDL muscle, a sensitive marker of lean mass catabolism, was smaller in LPCF mice at ∼9.9 mg/g compared to ∼11.1 and ∼10.9 mg/g in MPHF and HPHC groups,

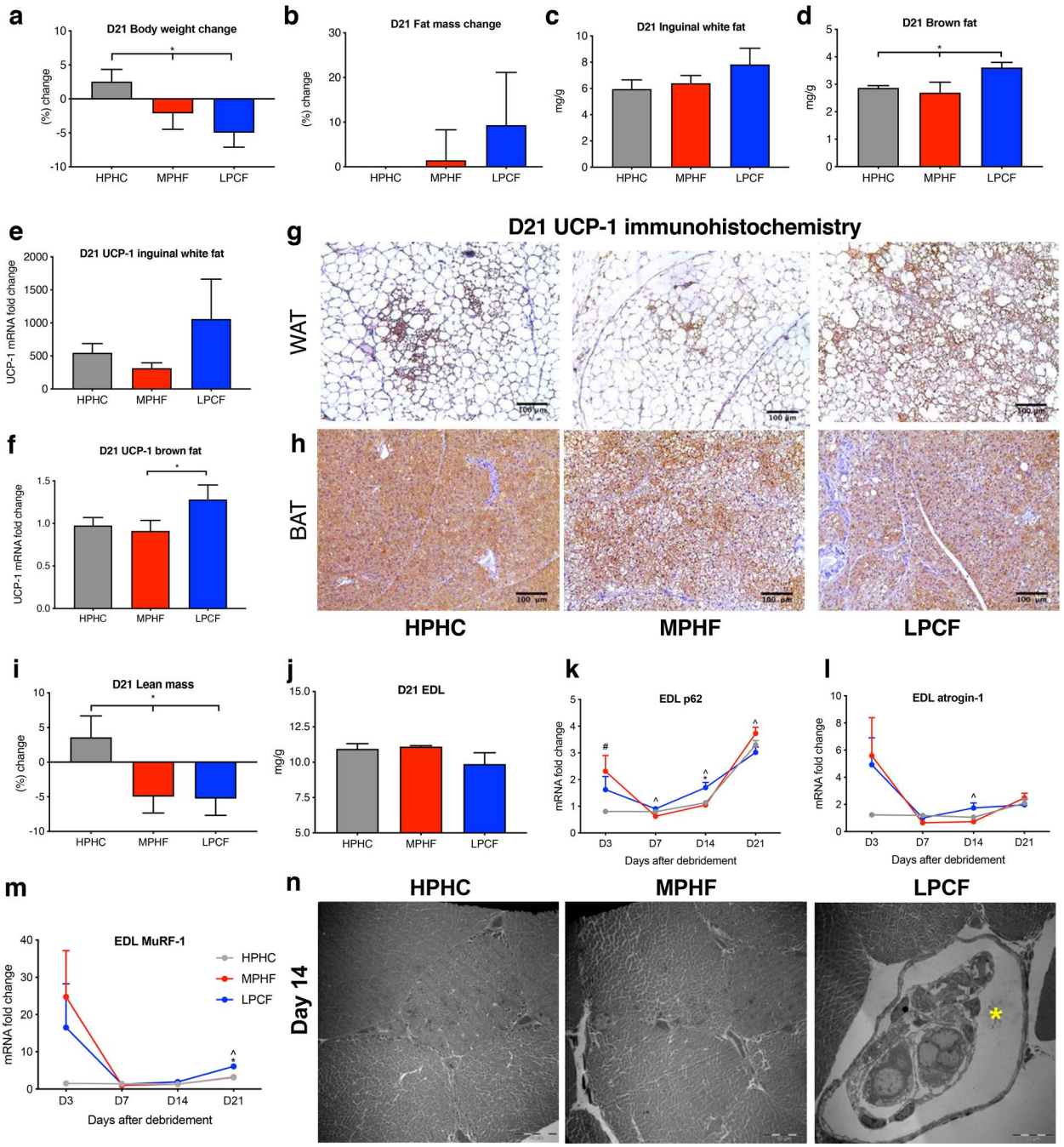

Figure 5. The effect of macronutrient intake on body fat and lean mass after full-thickness skin excision injury of mice. (**a**) Changes in body weight, (**b–d**) changes in fat mass, inguinal white adipose tissue (iWAT) and brown adipose tissue (BAT) mass in select diets on D21. (**e**, **f**) Uncoupling protein-1 (UCP-1) mRNA expression in iWAT and BAT on D21. (**g**, **h**) UCP-1 immunohistochemistry in iWAT and BAT, UCP-1 stains brown in multilocular adipocytes (scale bar = 100 μm). (**i**, **j**) Changes in lean mass and extensor digitorum longus muscle (EDL) on D21 in select diets. (**k–m**) p62, atrogin-1 and muscle-specific RING finger-1 (MuRF-1) mRNA expression throughout wound healing in select diets. (**n**) Representative transmission electron microscopy (TEM) images for D14 EDL in select diets, yellow star marks degenerate muscle fibres, (scale bar = 5 μm). $^{*}p \leq 0.05$ LPCF *vs* HPHC, $^{\wedge}p \leq 0.05$ LPCF *vs* MPHF, $^{\#}p \leq 0.05$ MPHF *vs* HPHC. Data presented as mean ± SEM, $n = 6$/diet (see also Table S3). *LPCF* low protein, equivalent carbohydrate and fat diet, *HPHC* high-protein, high-carbohydrate diet, *MPHF* moderate-protein, low-carbohydrate, high fat diet

respectively on D21 (Figure 5j). Autophagic processes, whereby cellular contents are degraded, recycled and made available for wound healing, were analyzed in EDL samples. The expression of p62, a mitochondrial protein that links ubiquitinated proteins to the autophagy machinery [13], was assessed. On D3, p62 mRNA expression was increased in both LPCF and MPHF mice but remained significantly elevated on D7 and D14 in LPCF mice, indicating increased

autophagy. On D21, p62 expression increased in all groups, but a significantly smaller increase was noted in LPCF mice (Figure 5k). Atrogin-1 and muscle-specific RING finger-1 (MuRF-1) are E3 ubiquitin ligase proteins that regulate ubiquitin protein degradation of muscle fibres [14]. A similar pattern to p62 expression was found with higher expression of atrogin-1 and MuRF-1 in the EDL muscle of LPCF and MPHF mice compared to HPHC. Interestingly, atrogin-1 mRNA expression was significantly increased in LPCF mice on D14 and MuRF-1 expression on D21 (Figure 5l and m). Transmission electron microscopy (TEM) analysis of EDL muscle showed no specific markers of autophagy in all select diets, but EDL muscle fibre degradation in LPCF mice was identified on D14 (Figure 5n) [15].

Discussion

The primary finding from this study is that a low-protein diet coupled with a balanced intake of carbohydrate and fat optimizes wound healing after skin excision in a mouse model. This finding was unexpected but significant in light of current clinical practice which encourages routine use of high-protein diets to support wound healing [7,8].

Locally, wound healing was accelerated in LPCF mice, and was associated with increased mRNA expression of essential cytokines, IL-6, TNF-α and TFG-β1. These cytokines regulate vital wound healing processes, in particular IL-6 increases leukocyte infiltration, re-epithelialization and collagen accumulation [16]. TNF-α is essential for inflammatory cell migration, fibroblast proliferation and angiogenesis [17]. TGF-β1, which was consistently higher in LPCF wounds, plays a predominant role in accelerating epithelial migration and promoting the progressive replacement of immature collagen III with mature collagen I [18]. This favourable cytokine expression was correlated with improved epidermal migration, cell proliferation and accelerated collagen deposition on histological analysis of LPCF mice wound tissue.

Systemically, LPCF mice had increased body fat mass, iWAT and BAT tissue. This result was expected as mice on low-protein diets generally consume more calories in an attempt to reach an essential protein intake target [19,20]. Excess energy intake can be expelled through enhanced thermogenesis, a process dependent on UCP-1, a mitochondrial protein, expressed predominantly in BAT and induced in iWAT with low-protein intakes and adrenergic stress [21]. LPCF mice had significantly greater energy expenditure and higher expression of UCP-1 mRNA in iWAT and BAT tissue. Previous research has shown that mice on a low-protein, high-carbohydrate diet with similar body fat changes observed in this study, had increased body surface temperature [22]. This is a potential mechanism by which a low-protein intake may improve wound healing by inducing thermogenesis, as heat improves circulation and accelerates local enzymatic processes [23].

Lean body mass loss was associated with low-protein and/or high-fat intakes and preserved with a high-protein intake. The ability of protein to preserve lean body mass is a well-known and studied phenomenon [6]. Preventing loss of lean body mass is important because considerable lean body mass loss has several negative effects including delayed wound healing, functional recovery and immunosuppression [24]. Interestingly, in this study, mice with a low-protein intake, although losing a small amount of lean body mass, had accelerated wound healing, suggesting that a degree of metabolism of endogenous protein from lean body mass rather than exogenous dietary protein is well tolerated and perhaps beneficial for wound healing [25]. This finding should be interpreted within the context of a skin excisional mouse model, as protein requirements in a mouse model of more severe stress, for example a burn injury, will likely be higher and the loss of lean body mass unlikely to be well tolerated.

LPCF mice had an early and brief systemic inflammatory response. On D3, IL-1, TNF-α and IL-6, which are potent cytokines for lean mass catabolism, were elevated in the serum of LPCF mice [19,24]. Supporting this finding, the EDL muscle in LPCF mice was lighter and the mRNA expression of E3 ligases atrogin-1 and MuRF-1 was increased. Together, these results suggest that low-protein intakes are associated with an early but short-lived inflammatory response that occurs simultaneously with optimal wound healing, suggesting endogenous protein reserves may be recycled for wound healing. One such process which is known to facilitate recycling of cellular protein is autophagy.

Autophagy is a well conserved house-keeping system that removes damaged cellular proteins for amino acid recycling and protein synthesis [20,26]. Previous experiments have confirmed that autophagy is inhibited by a high-protein intake while a high-carbohydrate intake seems to increase autophagy [13,25]. In LPCF mice, autophagy may be a process whereby damaged muscle proteins are recycled, increasing the amino acid pool available to the healing wound. This hypothesis was supported by increased p62 gene expression in the EDL of LPCF mice throughout the critical proliferative period of wound healing. Interestingly, a number of studies in critical care medicine have suggested patients receiving less protein had better outcomes, with autophagy being considered one possible explanation for these findings [27].

Healing depends on adequate flow of nutrients to the wound. Macronutrients may be sourced either endogenously from body stores or exogenously from dietary sources. Literature and research regarding optimal nutrition for wound healing has focused on exogenous dietary pathways and the effect of various macronutrient interventions, particularly high-protein diets. Through the GF, this study has identified a new concept, that stored body protein, mobilized from lean body mass, may be an important or even more important source of protein for the demanding cellular processes of wound healing. A low-protein diet, coupled with a balanced intake of carbohydrate and fat, triggered macronutrient-dependent processes including brown fat thermogenesis and autophagy, processes capable of accelerating wound healing.

Future research will focus on explaining how macronutrient intake can alter the breakdown of endogenous protein reserves and the effect this has on the amino acid profile available to healing tissue. Translation of this research into clinical dietary recommendation for post-surgery patients will require further investigation using animal models to first confirm underlying mechanisms, prior to assessing the effectiveness of high-energy, low-protein diets in human studies and developing medications that can directly influence these mechanisms to improve the release of endogenous stores of amino acids for wound healing. A possible avenue for conducting clinical trials is to assess the effectiveness of low-protein, balanced carbohydrate and fat intake in enhanced recovery after surgery (ERAS) protocols which commonly include dietary interventions to optimize healing [6,28,29].

Conclusions

The study highlights that a low-protein diet paired with a balanced carbohydrate and fat intake is the most favourable nutritional intervention for supporting acute cutaneous wound healing processes. Wounds healed faster in this dietary group, with evidence of enhanced collagen deposition and an early but short inflammatory response. UCP-1-dependent thermogenesis in brown and white adipose tissue and autophagy of lean body mass provide promising avenues for future research aimed at understanding systemic mechanisms governed by low-protein diets that accelerate local wound healing.

Supplementary material

Supplementary material is available at *Burns & Trauma Journal* online.

Abbreviations

BAT: Brown adipose tissue; C: Carbohydrate; CF: Carbohydrate and fat equivalent; EDL: Extensor digitorum longus muscle; F: Fat; GAM: Generalized additive models; GF: Geometric Framework; H&E: Haematoxylin and eosin; HPHC: High-protein, high-carbohydrate; HPHF: High-protein, high-fat; iWAT: Inguinal white adipose tissue; LPCF: Low-protein, equivalent carbohydrate and fat; MPHF: Moderate-protein, low-carbohydrate, high-fat; MuRF-1: Muscle-specific RING finger-1; P: Protein; PCNA: Proliferating cell nuclear antigen; TEM: Transmission electron microscopy; RQ: Respiratory exchange quotient; SIRS: Systemic inflammatory response syndrome

Authors' contributions

JJH, RJP, SMS-B, SJS, DGLC and YW designed study. JJH, CPM, JKS, CC, RJP, PS, RCFC, BA, SK, KH-YT, YW contributed to experiments. JJH, RJP and YW analyzed the data. JJH, RJP and YW wrote the paper. DGLC, ZL, PKM, SK, CN, SMS-B, MGJ and SJS assisted in the preparation of the manuscript. YW and PKM supervised the project.

Funding

This work was supported by the ANZAC Research Institute Seed Fund.

Conflict of interest

None declared.

Acknowledgements

JJH was supported by the John Loewenthal Scholarship. SMS-B was supported by a National Medical Health and Research Council of Australia Peter Doherty Early Career Fellowship (Grant 1110098). SJS was supported by an Australian Research Council Laureate Fellowship.

References

1. Brown KL, Phillips TJ. Nutrition and wound healing. *Clin Dermatol*. 2010;28:432–9.
2. Wild T, Rahbarnia A, Kellner M, Sobotka L, Eberlein T. Basics in nutrition and wound healing. *Nutrition*. 2010;26:862–6.
3. Dylewski ML, Yu YM. Protein and wound healing. In: Molnar JA (ed). *Nutrition and Wound Healing*. Florida: CRC press, 2007, 49–65.
4. Calder CP, Dimitriadis CG, Newsholme CP. Glucose metabolism in lymphoid and inflammatory cells and tissues. *Curr Opin Clin Nutr Metab Care*. 2007;10:531–40.
5. Turek JJ. Fat and wound healing. In: Molnar JA (ed). *Nutrition and wound healing*. Florida: CRC press, 2007, 27–48.
6. Demling RH. Nutrition, anabolism, and the wound healing process: an overview. *Eplasty*. 2009;9:65–94.
7. Stechmiller JK. Understanding the role of nutrition and wound healing. *Nutr Clin Pract*. 2010;25:61–8.
8. Weimann A, Braga M, Carli F, Higashiguchi T, Hubner M, Klek S, *et al*. ESPEN guideline: clinical nutrition in surgery. *Clin Nutr*. 2017;36:623–50.
9. Yoshino Y, Ohtsuka M, Kawaguchi M, Sakai K, Hashimoto A, Hayashi M, *et al*. The wound/burn guidelines - 6: guidelines for the management of burns. *J Dermatol*. 2016;43:989–1010.
10. Simpson SJ, Raubenheimer D. *The Nature of Nutrition: A Unifiying Framework from Animal Adaptation to Human Obesity*. Princeton: Princeton University Press, 2012.
11. Masters B, Arabi S, Sidhwa F, Wood F. High-carbohydrate, high-protein, low-fat versus low- carbohydrate, high-protein, high-fat ente1ral feeds for burns (review). *Cochrane Collaboration*. 2012;2:1–21.
12. Weir JBV. New method for calculating metabolic reate with special reference to protein metabolism. *J Biochem Physiol*. 1949;109:1–9.
13. Derde S, Vanhorebeek I, Guiza F, Derese I, Gunst J, Fahrenkrog B, *et al*. Early parenteral nutrition evokes a phenotype of autophagy deficiency in liver and skeletal muscle of critically ill rabbits. *Endocrinology*. 2012;153:2267–76.
14. Bodine SC, Baehr LM. Skeletal muscle atrophy and the E3 ubiquitin ligases MuRF1 and MAFbx/atrogin-1. *Am J Physiol Endocrinol Metab*. 2014;307:E469-84.
15. Mizushima N, Yoshimori T, Levine B. Methods in mammalian autophagy research. *Cell*. 2010;140:313–26.
16. Lin Z-Q, Kondo T, Ishida Y, Takayasu T, Mukaida N. Essential involvement of IL-6 in the skin wound-healing process as

evidenced by delayed wound healing in IL-6-deficient mice. *J Leukoc Biol*. 2003;73:713–21.
17. Gharaee-Kermani M, Phan SH. Role of cytokines and cytokine therapy in wound healing and fibrotic diseases. *Curr Pharm Des*. 2001;7:1083–103.
18. Alves CC, Torrinhas RS, Giorgi R, Brentani MM, Logullo AF, Waitzbery DL. TGF-β1 expression in wound healing is acutely affected by experimental malnutrition and early enteral feeding. *Int Wound J*. 2014;11:533–9.
19. Zamir O, Hasselgren P-O, Higashiguchi T, Frederick JA, Fischer JE. Tumor necrosis factor (TNF) and interleukin-1 (IL-1) induce muscle proteolysis through different mechanisms. *Mediators Inflamm*. 1992;1:247–50.
20. Patel JJ, Martindale RG, McClave SA. Controversies surrounding critical care nutrition: an appraisal of permissive underfeeding, protein, and outcomes. *JPEN J Parenter Enteral Nutr*. 2018;42:508–15.
21. Pezeshki A, Zapata RC, Singh A, Yee NJ, Chelikani PK. Low protein diets produce divergent effects on energy balance. *Sci Rep*. 2016;6:25145.
22. Huang X, Hancock DP, Gosby AK, McMahon AC, Solon SMC, Le Couteur DG, *et al*. Effects of dietary protein to carbohydrate balance on energy intake, fat storage, and heat production in mice. *Obesity*. 2013;21:85–92.
23. Leeds IL, Wick EC, Melton GB. Does close temperature regulation affect surgical site infection rates? *Adv Surg*. 2014;48:65–76.
24. Wray CJ, Mammen JMV, Hasselgren P-O. Catabolic response to stress and potential benefits of nutrition support. *Nutrition*. 2002;18:971–7.
25. Belghit I, Panserat S, Sadoul B, Dias K, Skiba-Cassy S, Seiliez I. Macronutrient composition of the diet affects the feeding-mediated down regulation of autophagy in muscle of rainbow trout. *PLoS One*. 2013;8:1–14.
26. Oczypok EA, Oury TD, Chu CT. It's a cell-eat-cell world. *Am J Pathol*. 2013;182:612–22.
27. Preiser J-C, van Zanten ARH, Berger MM, Biolo G, Casaer MP, Doig GS, *et al*. Metabolic and nutritional support of critically ill patients: consensus and controversies. *Crit Care*. 2015;19:35.
28. Huckleberry Y. Nutritional support and the surgical patient. *Am J Health-Syst Pharm*. 2004;61:671–84.
29. Medlin S. Nutrition for wound healing. *Br J Nurs*. 2012;21:S11–5.